








Original Research

Green synthesis of bis(indolyl)methane scaffolds as valuable biological materials catalyzed by $\text{Fe}_3\text{O}_4/\text{SiO}_2/\text{PPA}$ as a magnetic nanocatalyst

Fatemeh Chaltash¹ , Seyed Mohammad Vahdat^{1,*} , Roberto Acevedo² ,
Soheila Ghanbari³ , Mohammad Qandalee⁴ , Carlos J. Durán-Valle⁵ ,
Ignacio M. Lopez-Coca⁶ 

¹Department of Chemistry, Am.c., Islamic Azad University, Amol, Iran

²Universidad San Sebastián, Facultad de Ingeniería, Arquitectura y Diseño (FIAD), Bellavista 7. 8420524, Santiago, Chile

³Department of Analytical Chemistry, Faculty of Chemistry, K.N. Toosi University of Technology, Tehran, Iran

⁴Department of Basic Sciences, Ga.C. Islamic Azad University, Garmsar, Iran

⁵ACYS, Faculty of Sciences, Universidad de Extremadura, Badajoz, 06006, Spain

⁶INTERRA, School of Technology, Universidad de Extremadura, Caceres, 10003, Spain

*Corresponding author: sm.vahdat@iau.ac.ir

Article History

Received:
18 July 2025

Revised:
1 September 2025

Accepted:
18 September 2025

Published online:
12 October 2025

Published in Issue:
10 April 2026

© 2026 The Author(s). Published by the OICC Press under the terms of the CC BY 4.0, Creative Commons Attribution License, which permits use, distribution and reproduction in any medium, provided the original work is properly cited.

Abstract:

This study applied $\text{Fe}_3\text{O}_4/\text{SiO}_2/\text{PPA}$ magnetic nanocatalyst as a solid acid catalyst to produce bis(indolyl)methane derivatives (BIMs) under solvent-free conditions and at 50 °C. FTIR, XRD, EDX, FESEM, HRTEM, and BET were used for structure confirmation. The catalyst was environmentally friendly, heterogeneous, and recyclable without loss of catalytic activity. Also, this catalyst had high efficiency for the synthesis of bis(indolyl) methanes and the reaction products were obtained quickly. The synthesis of bis(indolyl)methanes from the reaction between indole derivatives and aldehydes has been carried out in short reaction times (5 – 30 min) with good to excellent yields (65 – 96%) using 50 mg of magnetic nanocatalyst at solvent-free conditions.

Keywords: Biological materials; Bis(indolyl)methanes; $\text{Fe}_3\text{O}_4/\text{SiO}_2/\text{PPA}$; Indole; Magnetic nanocatalyst; Solvent free

Cite this article: Chaltash F, Vahdat SM, Acevedo R, Ghanbari S, Qandalee M, Durán-Valle CJ, Lopez-Coca IM. Green synthesis of bis(indolyl)methane scaffolds as valuable biological materials catalyzed by $\text{Fe}_3\text{O}_4/\text{SiO}_2/\text{PPA}$ as a magnetic nanocatalyst. Int. J. Nano Dimens. 2026;17(2): 218-237. <https://doi.org/10.57647/j.ijnd.2026.1702.07>

1. Introduction

Indole and its derivatives are critical heterocyclic molecules which have intrigued organic chemists for many years. These scaffolds exhibit biological solid features, such as antibacterial, cytotoxic, anti-inflammatory, and anti-leishmanial actions [1, 2, 3, 4, 5, 6]. Indole is an electron-rich heteroaromatic system. This compound

shows high nucleophilic reactivity for electrophilic alkylation at the C3 and C2 positions of theazole ring. In this study, we investigated the reactivity of the C-3 atom of indoles in electrophilic reactions. The presence of a non-bonding electron pair on nitrogen and the conjugation of this electron pair with the double bond C=C in theazole ring make the carbon 3 position in the ring

electron-rich and act as a good nucleophilic site for attack by electrophilic groups including carbonyl aldehydes. Various studies confirm the existence of 3-substituted indole derivatives [7, 8, 9, 10, 11, 12, 13, 14, 15, 16].

Bisindolylmethanes (BIMs) have an indole heterocycle as a core unit in their chemical structures. These derivatives can be extracted from bioactive alkaloids of both terrestrial and marine origin [17]. The indole tag is the most common structure in bioactive alkaloids. These structures are highly active cruciferous scaffolds used to develop valuable estrogen metabolism and suppress apoptosis in human cancer cells [18]. BIMs show diverse anticancer activities that effectively prevent the proliferation of various types of cancer cells, including bladder, cervical, colon and prostate [19, 20]. Additionally, these compounds possess notable anti-HIV properties [21].

In this study, and because of the importance of reactions catalyzed by solid acid-based catalysts, a plant species was used as a new organic source for the synthesis of this type of catalyst for the first time. Acid catalysts are generally classified into two major groups, homogeneous and heterogeneous acid catalysts. There are several homogeneous organic and inorganic materials that act as Lewis or Brønsted-Lowry acids and are efficient in organic reactions [22, 23, 24, 25]. On the other hand, in recent years, there has been great interest in using heterogeneous (solid) acid catalysts instead of homogeneous catalysts due to the possibility of recovering and recycling solids, which leads to a reduction in environmental impacts. Also, most solid-state acids are heterogeneous organic acids and transition metal complexes [26, 27, 28].

Despite the widespread use of organic and inorganic acid catalysts, the leakage of hazardous acids into the target product is one of the negative aspects of using heterogeneous acid-based catalysts in stable catalysts [29]. To overcome this problem, coupling homogeneous acid catalysts with heterogeneous catalytic materials, as novel and efficient solid acid catalysts, seems to be a suitable solution [24, 28]. What we are pursuing in this research.

In recent years, the essential catalysts employed in the synthesis of bis-indolylmethane derivatives include several SO_3H ILs [30], $\text{AIPW}_{12}\text{O}_{40}$ [31], [PCBS] and [TCBDA] [32], $\text{Cu}_{1.5}\text{PMo}_{12}\text{O}_{40}$ [33], [Fe(III)(salen)]Cl [34], PEG-supported sulfonic acid [35], TiO_2 nanoparticles [36], PSFSI/SBA-15 [37], $[\text{MIMPS}]_3\text{PW}_{12}\text{O}_{40}$ and $[\text{TEAPS}]_3\text{PW}_{12}\text{O}_{40}$ [38] and catalyst-free condition [39].

However, the prevalent catalysts and methods for the synthesis of bisindolylmethanes have several drawbacks, which create significant limitations. Key drawbacks include prolonged reaction times, harsh conditions required for product separation, temperatures, complex synthetic pathways, use of halide- and metal-containing catalysts, cost catalysts, toxic solvents, diminished catalytic activity, low solubility and the presence of impurities in the final products.

A promising approach to reduce these issues is the

utilization of environmentally friendly catalysts. The use of plant-derived organic materials for the synthesis of these green catalysts increases the stability and facilitates the recycling of the catalyst through simple and cost-effective processes. This study used the perennial *Equisetum arvense* to synthesize a silicon-rich green catalyst. In *Equisetum arvense*, silica is mainly present in amorphous form. The high content of silica in this species has potential applications in medicinal chemistry. In addition to silicon and silicate, *Equisetum arvense* contains minerals and valuable elements such as potassium, calcium, aluminum, sulfur, magnesium, manganese, zinc, chromium and cobalt which increase its utility [40, 41, 42, 43, 44].

On the other hand, magnetic nanoparticles play an important role in different substrates due to their magnetic properties, high stability and catalytic activity. They also allow cost-effective and simple recovery using an external magnet, making them suitable for heterogeneous catalysis [45, 46, 47, 48, 49, 50, 51]. The development of environmentally friendly methods for the preparation of heterogeneous catalysts led us to focus our research on the use of horsetail as a source of biosilica (figure 1) for the stabilization of concentrated polyphosphoric acid ($\text{Fe}_3\text{O}_4/\text{SiO}_2/\text{PPA}$) (figure 2).



Figure 1. Image of horsetail plant [52].

This study aims to utilize a plant as a sustainable,

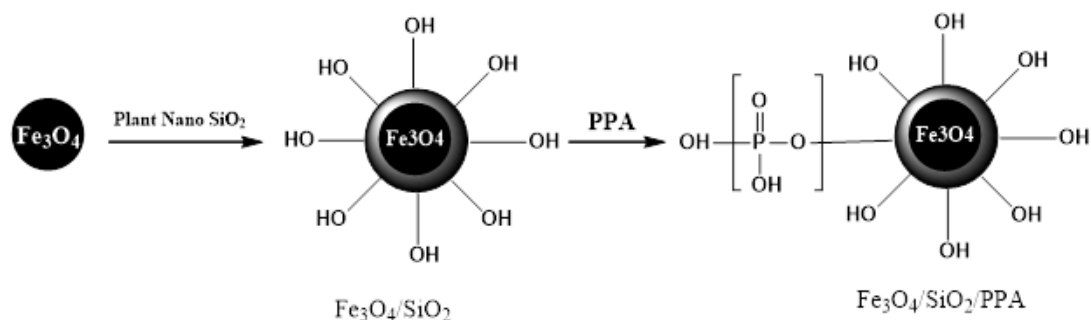


Figure 2. Preparation of $\text{Fe}_3\text{O}_4/\text{SiO}_2/\text{PPA}$ magnetic nanocatalyst.

eco-friendly and organic source to produce derivatives with extensive chemical and medicinal applications. We employed carbonyl compounds derived from aldehyde (1) and indole or 2-methylindole (2), applying the $\text{Fe}_3\text{O}_4/\text{SiO}_2/\text{PPA}$ magnetic nanocatalyst as a biocatalyst. Ultimately, this approach facilitates the synthesis of bis(indolyl)methanes (3), as illustrated in figure 3.

2. Experimental

2.1 Materials and methods

Solvents and materials were acquired from commercial providers and utilized as received. FE-SEM images were captured using a Tescan MIRA2 (Czech Republic). The structures of the crystal were analyzed by X-ray diffraction (XRD) on a PW1730-PHILIPS diffractometer with $\text{Cu K}\alpha$ radiation ($\lambda = 1.56056 \text{ \AA}$) at 40 keV. The FT-IR spectra using a Nicolet 300 spectrophotometer were obtained. HRTEM spectra were captured by an FEI Tecnai G2 F20 Super T win TEM spectrometer (200 kV) from FEI (USA). EDS assessed the elemental composition of the samples from SAMX (France). The surface area, pore volume and average pore diameter were determined using a BELSORP MINI. Surface areas were calculated via nitrogen gas adsorption at 77 K utilizing the Brunauer–Emmett–Teller (BET) method. At the same time, pore size distribution was assessed using Barrett–Joyner–Halenda (BJH) and Dollimore–Heal (DH) methods. Proton nuclear magnetic resonance (^1H NMR) spectra were obtained at $\delta \sim 2.5$ ppm and 3.5 ppm for DMSO-d_6 , or $\delta \sim 0.00$ ppm for TMS as a reference, while carbon nuclear magnetic resonance (^{13}C NMR) spectra were captured on a DRX spectrometer (100 MHz), with the solvent's chemical shift at $\delta \sim 40.0$ ppm for DMSO-d_6 as a reference.

2.2 Preparation of nano-silica from *Equisetum arvense*

20 g of dried plant was mixed with 100 mL of HCl (1N) solution in a 250 mL flask. The reaction mixture was refluxed for 1.5 h. Then it was soaked in acid at room temperature (20 hours). The mixture was filtered, and washed several times with hot distilled water (monitored with pH paper to completely remove the acid). The wet solid was placed in an oven at a temperature of 110 °C (24 hours) to dry and turn into ash. At the end, in order to prepare plant nano-silica, the dried sample was placed in an oven with a temperature of 700 °C for one hour to prepare nano-silica directly from plant ash.

2.3 Preparation of silica (from *Equisetum arvense* plant) coated on Fe_3O_4 nanoparticles

In a 250 mL flask, 1 g of nano Fe_3O_4 added to 80 mL of ethanol. Then 20 mL deionized water and 2 mL of 28% ammonia solution added to the resulting suspension (if the solution is not single-phase, the solution can be ultrasonicated for half an hour to make the solution single-phase and homogeneous). Then 0.2 g of plant ash prepared in the previous step was added and let it stir for 24 hours. The product was filtered, separated with a magnet, washed three times with deionized water and dried in an oven at 50–60 °C for a maximum of 12 hours [53].

2.4 Preparation of $\text{Fe}_3\text{O}_4/\text{SiO}_2$ -supported polyphosphoric acid as catalyst

1 g of $\text{Fe}_3\text{O}_4/\text{SiO}_2$ was added into 10 mL of methanol, followed by the addition of 1 g of polyphosphoric acid (PPA) to the resulting suspension. The mixture underwent ultrasonication and the solvent was subsequently evaporated under reduced pressure. The $\text{Fe}_3\text{O}_4/\text{SiO}_2/\text{PPA}$ catalyst was then placed in an oven at 100 °C for 3 hours to ensure thorough drying.

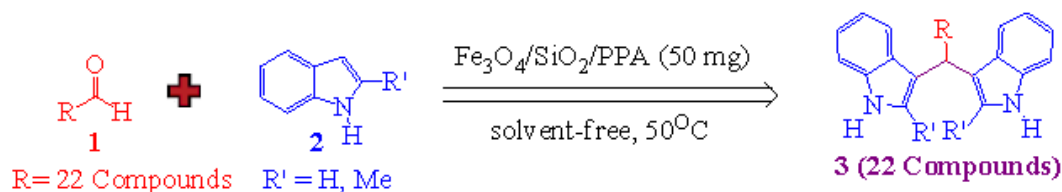


Figure 3. Synthesis of bis(indolyl)methanes catalyzed by $\text{Fe}_3\text{O}_4/\text{SiO}_2/\text{PPA}$ magnetic nanocatalyst.

2.5 General procedure for the synthesis of bis(indolyl)methanes

A total of 1 mmol of various aldehydes was reacted with 2 mmol of indole or 2-methylindole in the presence of 0.05 g of Fe₃O₄/SiO₂/PPA catalyst under solvent-free conditions at a temperature of 50 °C. The progress of the reaction was tracked by thin layer chromatography (TLC), utilizing an appropriate solvent ratio of n-hexane and ethyl acetate (1:5). Upon reaction completion, as the catalyst was insoluble in ethanol while the reaction mixture was soluble, a small amount of ethanol was added to the reaction mixture, allowing the catalyst to be separated magnetically. The resulting products were purified by recrystallization in a minimal amount of hot ethanol followed by n-hexane.

2.6 Selected spectral data analysis for compounds

3,3'-((4-nitrophenyl)methylene)bis(2-methyl-1H-indole) (Entry 2):

¹H NMR (400 MHz, DMSO): δppm = 10.90 (s, 2H, -NH), 8.17 (d, 2H, Ar-H), 7.44 (d, 2H, Ar-H), 7.26 (d, 2H, Ar-H), 6.93 (t, 2H, Ar-H), 6.82 (d, 2H, Ar-H), 6.72 (t, 2H, Ar-H), 6.09 (s, 1H, CH aliphatic), 2.13 (s, 6H, 2Me). ¹³C NMR spectrum (100 MHz, DMSO-d₆): δppm = 12.4, 39.2, 111.0, 111.3, 118.7, 118.8, 120.2, 123.7, 128.4, 130.3, 133.1, 135.6, 146.2, 153.4.

3,3'-((thiophen-2-ylmethylene)bis(2-methyl-1H-indole) (Entry 3):

¹H NMR (400 MHz, DMSO): δppm = 10.82 (s, 2H, -NH), 6.73-7.35 (m, 11H, Ar-H), 6.14 (s, 1H, CH aliphatic), 2.18 (s, 6H, 2Me). ¹³C NMR spectrum (100 MHz, DMSO-d₆): δppm = 12.4, 34.6, 110.8, 113.0, 118.5, 118.9, 120.1, 124.5, 125.5, 126.9, 128.2, 132.4, 135.4, 149.7.

3,3'-((4-methoxyphenyl)methylene)bis(2-methyl-1H-indole) (Entry 4):

¹H NMR (400 MHz, DMSO): δppm = 10.74 (s, 2H, -NH), 7.22 (d, 2H, Ar-H), 7.10 (d, 2H, Ar-H), 6.82-6.91 (m, 6H, Ar-H), 6.69 (t, 2H, Ar-H), 5.88 (s, 1H, CH aliphatic), 3.72 (s, 3H, OMe) 2.08 (s, 6H, 2Me). ¹³C NMR spectrum (100 MHz, DMSO-d₆): δppm = 12.4, 38.2, 55.4, 110.8, 113.0, 113.7, 118.4, 119.0, 119.9, 128.7, 130.0, 132.4, 135.5, 136.6, 157.8.

3. Results and discussions

3.1 Characterization of catalyst

3.1.1 FT-IR analysis of the catalyst

Figure 4 presents the FT-IR spectra of plant-derived nanosilica (4 a), Fe₃O₄/SiO₂ (4 b), and the synthesized Fe₃O₄/SiO₂/PPA catalyst (4 c). In figure 4 a, the absorption band at 3462 cm⁻¹ corresponds to the stretching vibrations of the Si-OH bond [54, 55]. The absorption band at 1573 cm⁻¹ is attributed to the bending vibrations of water molecules [41]. A strong absorption band at 1098 cm⁻¹ is associated with the asymmetric Si-O-Si stretching vibrations in the siloxane bond structure, while bands at 792 cm⁻¹ and 642 cm⁻¹ correspond to symmetric Si-O-Si stretching vibrations. The absorption band at

470 cm⁻¹ also confirms the Si-O-Si bending vibrations [54].

In figure 4 b, an absorption band at 563 cm⁻¹ is observed alongside the above signals, corresponding to the Fe-O bond vibration in Fe₃O₄, verifying the formation of magnetic nanosilica [56].

In figure 4 c, in addition to the previously mentioned signals, an absorption band at 1012 cm⁻¹ is attributed to the phosphate group, confirming that this group has been successfully placed on the Fe₃O₄/SiO₂ structure, indicating the successful synthesis of the Fe₃O₄/SiO₂/PPA catalyst [56].

3.1.2 X-ray powder diffraction pattern (XRD) analysis of the catalyst

Figure 5 illustrates the X-ray powder diffraction (XRD) patterns for plant-derived nanosilica (5 a), Fe₃O₄/SiO₂ (5 b), and the synthesized Fe₃O₄/SiO₂/PPA catalyst (5 c). In 5 a, the prominent peak at 2θ = 22.5° along with the weak peaks in the 30° – 40° range, confirms the successful synthesis of nanosilica in the catalyst [57].

In 5 b, the presence of three weak peaks within the 30°–40° range further supports the incorporation of nanosilica in the synthesized catalyst [57]. Additionally, distinct and sharp peaks observed at 2θ values of 31°, 35°, 43°, 54°, 57°, and 63° are indicative of the presence of nano Fe₃O₄ within the structure [58].

Similarly, in 5 c, the peak at 2θ = 22.5°, along with three weak peaks in the 30° – 40° range, confirms the presence of nanosilica in the Fe₃O₄/SiO₂/PPA catalyst. The clear and sharp diffraction peaks at 31°, 35°, 43°, 54°, 57°, and 63° confirm the existence of nano Fe₃O₄ within the synthesized catalyst [58]. These results align with standard reference data and confirm the crystalline structure of the synthesized catalyst.

3.1.3 EDX analysis of the catalyst

The elemental composition of the Fe₃O₄/SiO₂ and Fe₃O₄/SiO₂/PPA samples were analyzed using energy-dispersive X-ray spectroscopy (EDX) and elemental mapping as demonstrated by the EDX analysis and mapping results presented in figure 6 (for the Fe₃O₄/SiO₂ compound) and figure 7, Table 1 (for the Fe₃O₄/SiO₂/PPA catalyst). In figure 6, the presence of Fe, O and Si elements in the Fe₃O₄/SiO₂ compound is clearly confirmed.

In figure 7 and Table 1, the presence of Fe, O, Si, and P elements in the Fe₃O₄/SiO₂/PPA catalyst is clearly confirmed. This indicates that polyphosphoric acid (PPA) was successfully incorporated on the Fe₃O₄/SiO₂ substrate in the final step of the synthesis, verifying the successful preparation of the catalyst.

3.1.4 FESEM and HRTEM analysis of the catalyst

The structural characteristics of Fe₃O₄/SiO₂/PPA magnetic nanoparticles were investigated using transmission electron microscopy (TEM) and field emission scanning electron microscopy (FE-SEM). The catalyst exhibits a uniform and continuous morphology, with an average particle size of approximately 63 nm, as observed in the FE-SEM analysis, and a particle diameter ranging from

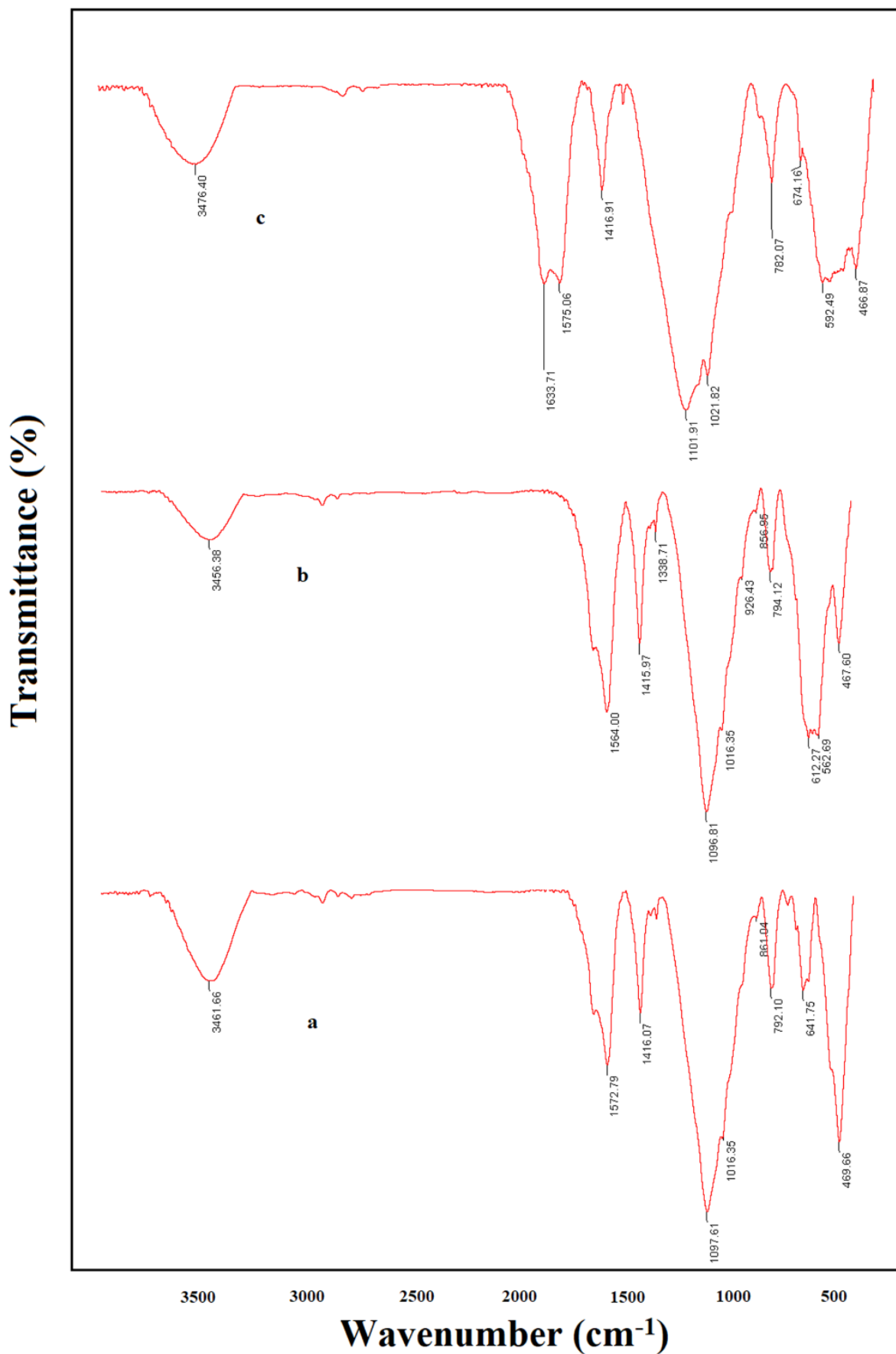


Figure 4. FTIR spectra of plant nanosilica (a), Fe₃O₄/SiO₂ (b) and synthesized Fe₃O₄/SiO₂/PPA catalyst (c).

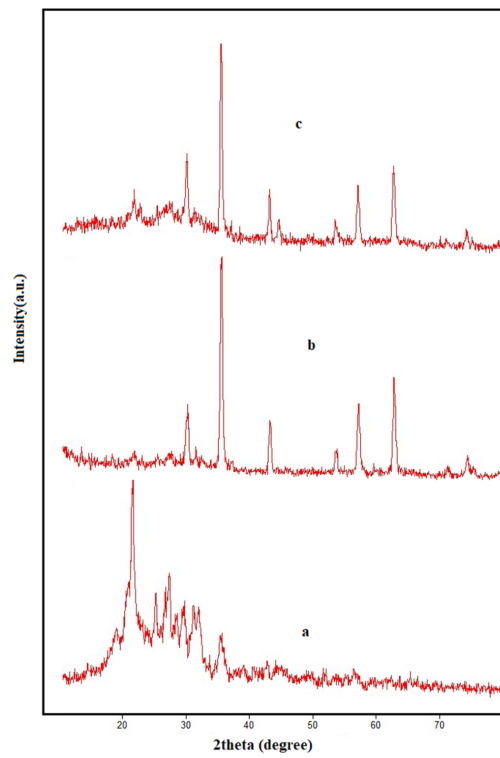


Figure 5. XRD spectra of plant nanosilica (a), Fe₃O₄/SiO₂ (b) and synthesized Fe₃O₄/SiO₂/PPA catalyst (c).

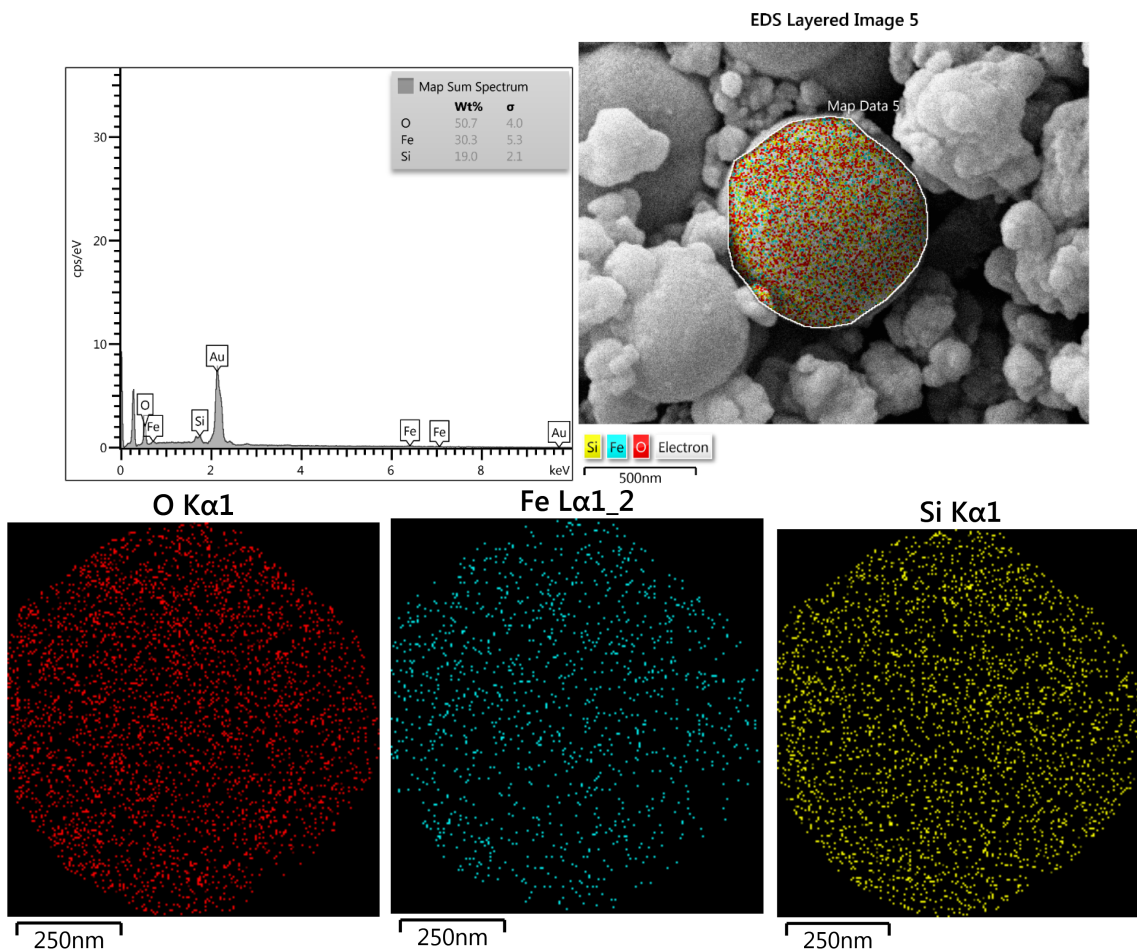


Figure 6. The EDX spectroscopy analysis and mapping figures of the Fe₃O₄/SiO₂ material.

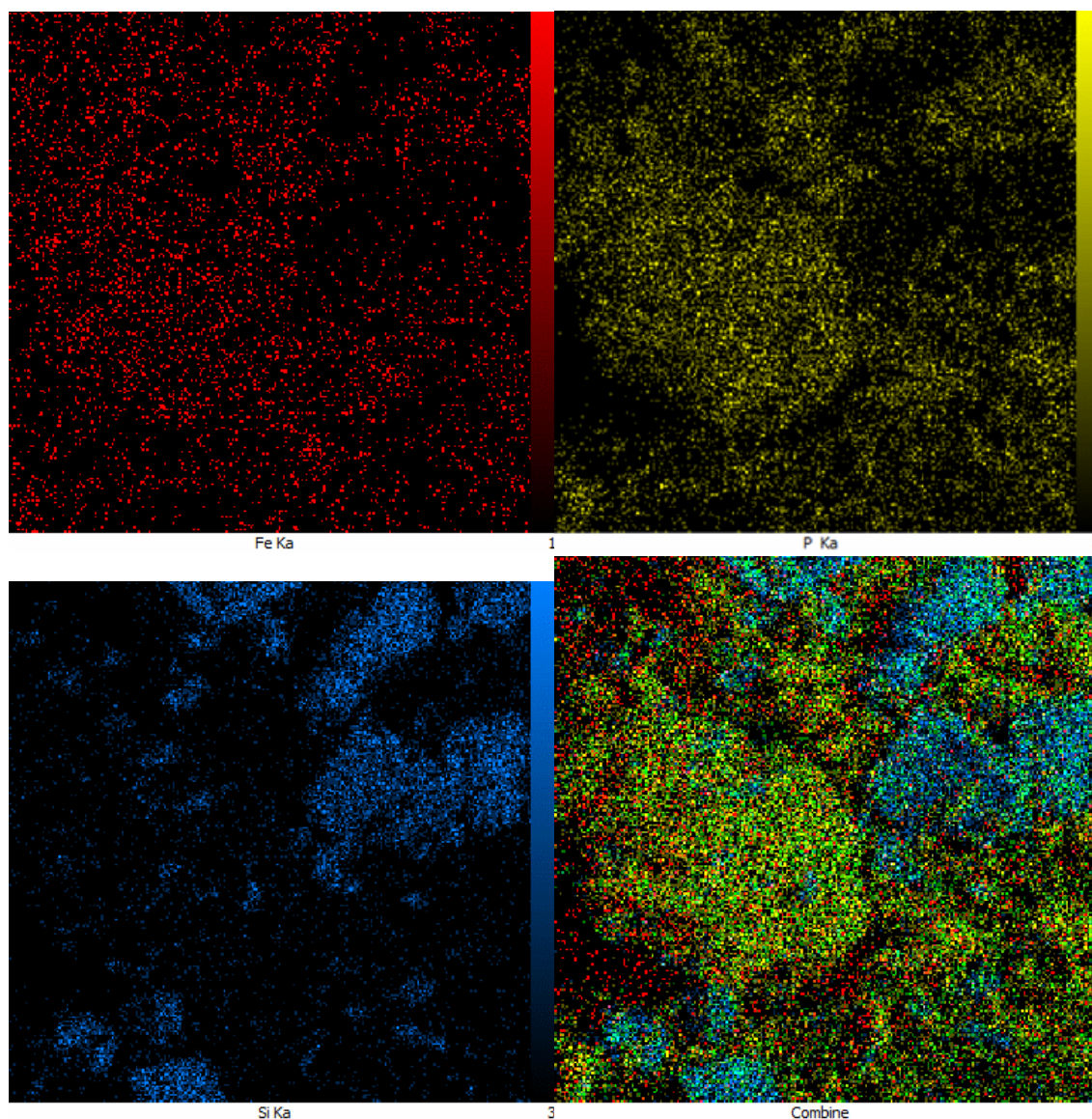


Figure 7. The mapping figures of the $\text{Fe}_3\text{O}_4/\text{SiO}_2/\text{PPA}$ catalyst.

10 to 20 nm in the HRTEM images (figures 8 and 9).

3.1.5 BET analysis of the catalyst

The specific surface area, pore volume, and average pore diameter of the $\text{Fe}_3\text{O}_4/\text{SiO}_2/\text{PPA}$ composite are presented in Table 2. A thorough analysis of the data

in Table 2 reveals that due to the removal of organic constituents from the plant material, the elevated levels of horsetail ash, produced at high temperatures contribute to an increase in both pore volume and mean pore diameter of the synthesized catalyst. This modification is likely to enhance the catalytic efficiency and shorten the reaction

Table 1. The EDX spectroscopy analysis of the $\text{Fe}_3\text{O}_4/\text{SiO}_2/\text{PPA}$ catalyst.

Elt	Line	Int	Error	K	Kr	W%	A%	ZAF	Formula	Ox%	Pk/Bg	Class	LConf	HConf	Cat#
O	Ka	225.8	36.1263	0.3973	0.2418	53.73	72.13	0.4501		0.00	69.74	A	52.43	55.03	0.00
Mg	Ka	7.9	0.5410	0.0050	0.0030	0.55	0.48	0.5540		0.00	2.59	B	0.48	0.62	0.00
Si	Ka	202.7	3.6365	0.1307	0.0796	10.15	7.76	0.7841		0.00	13.88	A	9.89	10.41	0.00
P	Ka	297.8	3.6365	0.2184	0.1329	17.50	12.13	0.7597		0.00	22.84	A	17.13	17.87	0.00
K	Ka	11.6	0.6328	0.0129	0.0079	0.92	0.50	0.8571		0.00	3.27	B	0.82	1.02	0.00
Ca	Ka	30.0	0.6328	0.0373	0.0227	2.54	1.36	0.8923		0.00	4.85	A	2.37	2.71	0.00
Fe	Ka	64.9	0.6510	0.1984	0.1208	14.61	5.62	0.8264		0.00	12.83	A	13.95	15.27	0.00
				1.0000	0.6087	100.00	100.00			0.00					0.00

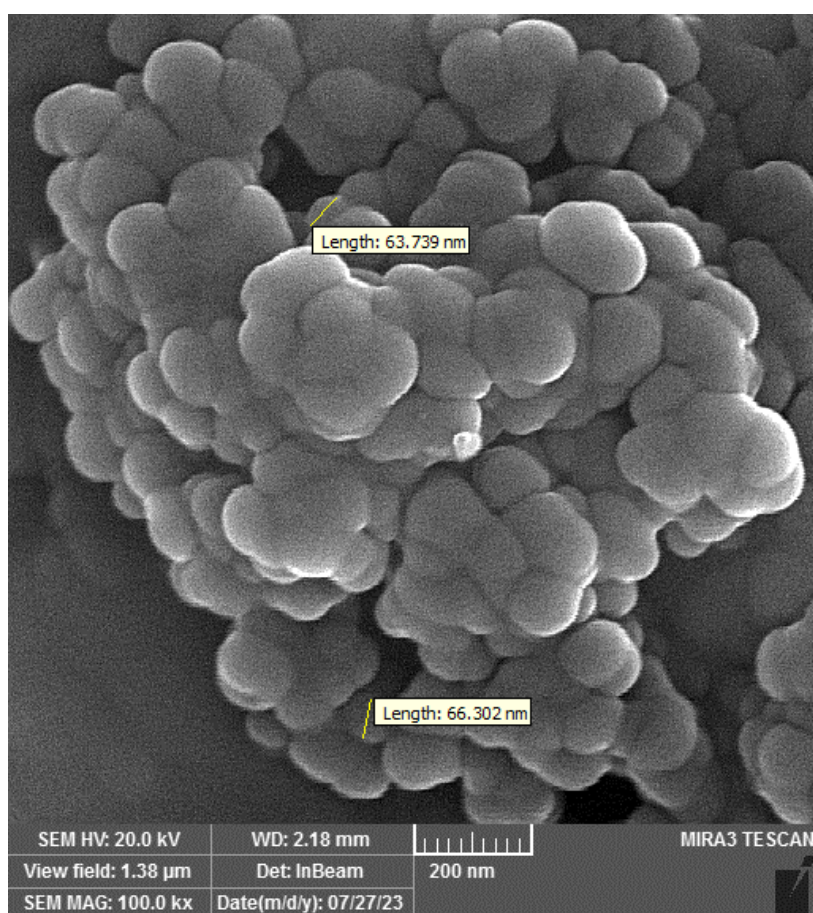


Figure 8. FE-SEM image of $\text{Fe}_3\text{O}_4/\text{SiO}_2/\text{PPA}$ magnetic nanoparticles.

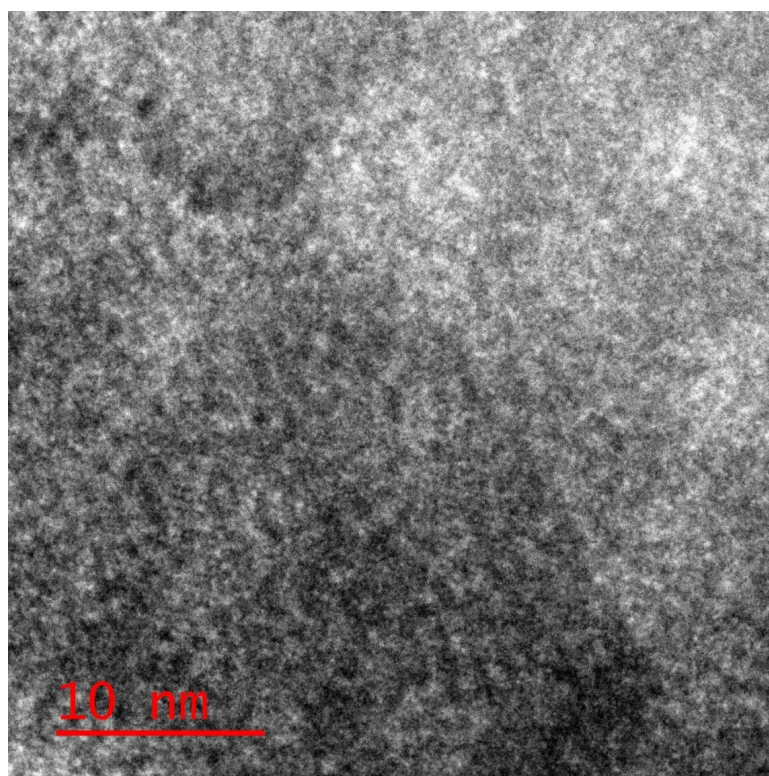


Figure 9. HRTEM image of $\text{Fe}_3\text{O}_4/\text{SiO}_2/\text{PPA}$ magnetic nanoparticles.

Table 2. The specific surface area, pore volume and mean pore diameter for Fe₃O₄/SiO₂/PPA.

	BET plot	
V _m	0.4532	cm ³ (STP)g ⁻¹
a _{s,BET}	1.9727	m ² g ⁻¹
C	47.018	
Total pore volume (<i>p/p</i> ₀ = 0.990)	0.035397	cm ³ g ⁻¹
Mean pore diameter	71.774	nm

time in the synthetic process.

3.2 Catalytic tests

3.2.1 Effect of various solvents on the reaction progress

In order to establish the optimal solvent for the reaction or to assess the feasibility of solvent-free conditions, the reaction was evaluated across various solvents and under solvent-free conditions. The model reaction (4-nitrobenzaldehyde and indole) was tested using ethanol, methanol, distilled water, chloroform, dichloromethane, ethyl acetate, toluene and acetone solvents as well as solvent-free conditions. The results showed that, fortunately, the case without solvent was placed in ideal conditions and the best efficiency and the shortest reaction time were obtained. Also, by increasing the temperature from 30 °C to 50 °C, the reaction efficiency increased and the reaction time decreased and increasing the temperature to 60 °C did not affect the reaction

efficiency (Table 3). Also, among the solvents used, ethanol had the best performance and was placed after the solvent-free conditions. While the use of toluene, acetone, methanol, ethyl acetate, distilled water, chloroform and dichloromethane solvents decreased the reaction efficiency compared to the solvent-free conditions.

3.2.2 Studying the impact of catalyst amount on the condensation reaction

The model reaction (4-nitrobenzaldehyde and indole) was selected to determine the optimal catalyst amount under solvent-free conditions at 50 °C. The results demonstrated that increasing the catalyst quantity from 0.001 g to 0.05 g improved reaction efficiency and reduced reaction time. However, further increases in catalyst amount beyond 0.05 g had no significant effect on either efficiency or reaction time (Table 4). Consequently, 0.05 g was identified as the optimal catalyst amount, as it yielded

Table 3. Optimization of the reaction conditions in model reaction (4-nitrobenzaldehyde and indole)^a.

Entry	Solvent	Temp. (°C) (under reflux)	Reaction time (min)	Yield (%) ^b
1	EtOH	78	5	84
2	MeOH	65	60	44
3	H ₂ O	100	6	83
4	CHCl ₃	60	90	47
5	CH ₂ Cl ₂	40	20	35
6	Ethyl acetate	77	20	78
7	Toluene	110	10	66
8	Acetone	56	15	43
9	—	30	10	71
10	—	40	7	86
11	—	50	5	92
12	—	60	5	92

^aReaction conditions: 4-nitrobenzaldehyde (1.0 mmol), Indol (2.0 mmol), and Fe₃O₄/SiO₂/PPA magnetic nanocatalyst (50 mg), at 50 °C;

^bIsolated yield.

Table 4. Optimization of the catalyst amount in model reaction^a.

Entry	Amount of catalyst (g)	Time (min)	Yield (%) ^b
1	0.001	20	69
2	0.005	17	76
3	0.01	12	87
4	0.05	5	92
5	0.1	5	92
6	0.2	5	92

^aReaction conditions: 4-nitrobenzaldehyde (1.0 mmol), Indol (2.0 mmol), and Fe₃O₄/SiO₂/PPA magnetic nanocatalyst (50 mg), at 50 °C;

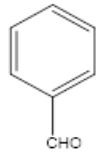
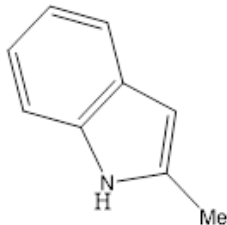
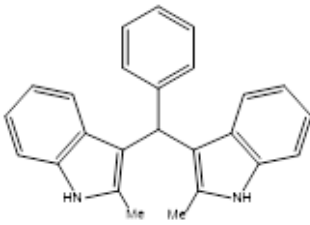
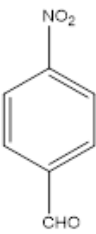
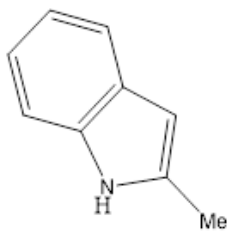
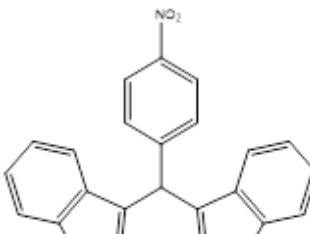
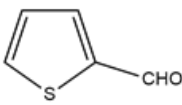
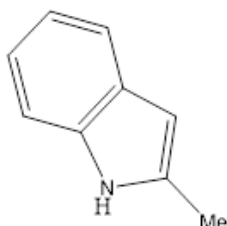
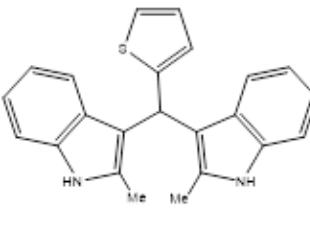
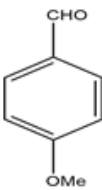
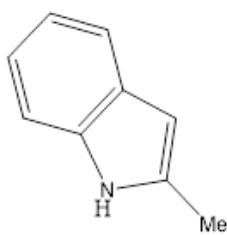
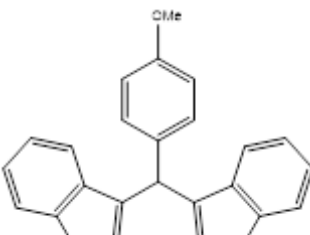
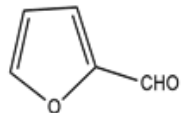
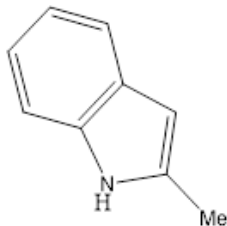
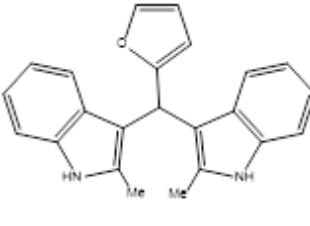
^bIsolated yield.

maximum efficiency in the shortest reaction time.

After establishing the optimal reaction conditions, indole and 2-methylindole were employed as starting materials to synthesize a series of bis(indolyl)methane

derivatives using aldehydes containing either electron-withdrawing or electron-donating groups, as well as heteroaromatic aldehydes. The results, presented in [Table 5](#), indicate that various substituted benzaldehydes

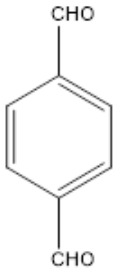
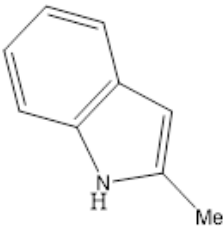
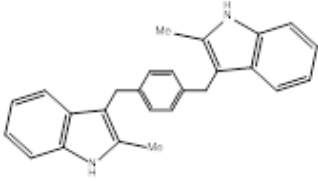
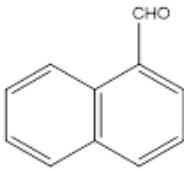
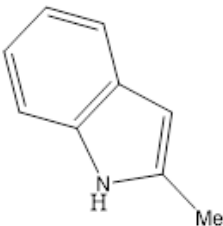
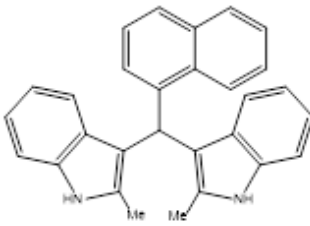
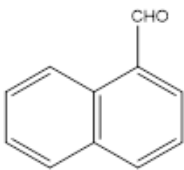
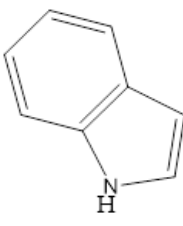
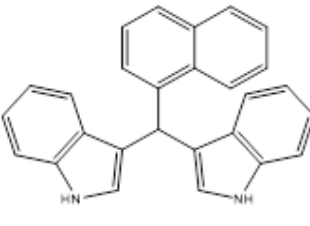
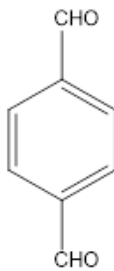
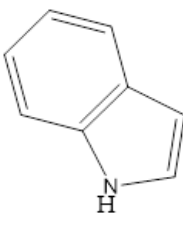
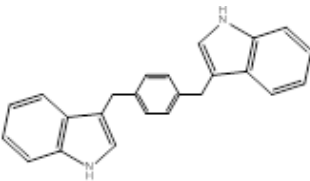
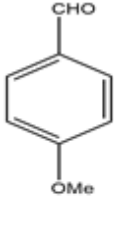
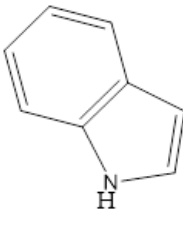
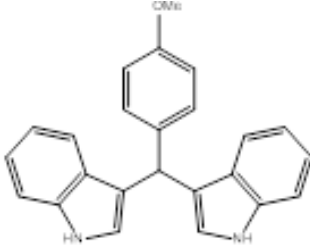
Table 5. Synthesis of bis(indolyl)methane compounds in the presence of $\text{Fe}_3\text{O}_4/\text{SiO}_2/\text{PPA}$ magnetic nanocatalyst (50 mg) under solvent-free conditions at $50\text{ }^\circ\text{C}$.^{a, b}

Entry	Aldehyde	2-Methylindol And Indol	Product	Time (min)	Yield (%)
1				15	70
2				10	73
3				15	94
4				30	65
5				10	92

^aReaction conditions: aldehyde (1 mmol), indole or 2-methylindole (2 mmol), $\text{Fe}_3\text{O}_4/\text{SiO}_2/\text{PPA}$ magnetic nanocatalyst (50 mg), solvent-free conditions, at $50\text{ }^\circ\text{C}$;

^bIsolated yield.

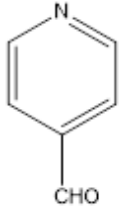
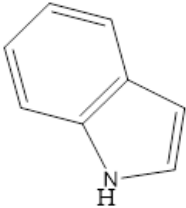
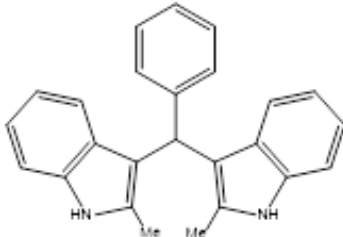
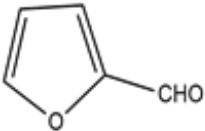
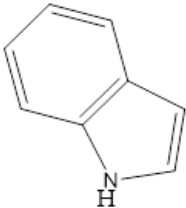
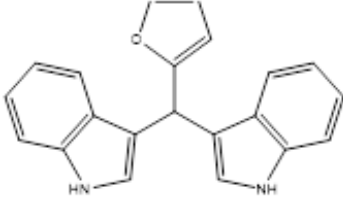
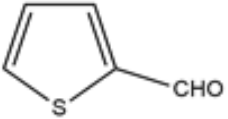
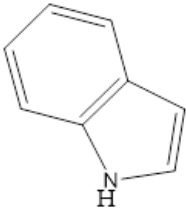
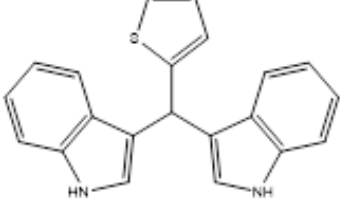
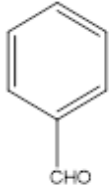
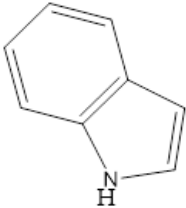
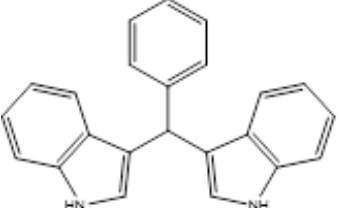
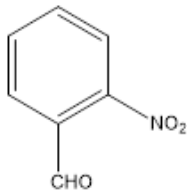
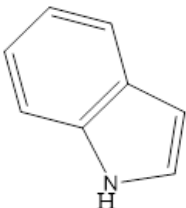
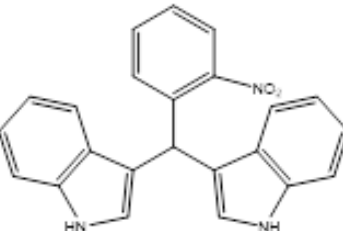
Continued of Table 5.

Entry	Aldehyde	2-Methylindol And Indol	Product	Time (min)	Yielda (%)
6				8	76
7				10	88
8				10	86
9				8	76
10				8	76

^aReaction conditions: aldehyde (1 mmol), indole or 2-methylindole (2 mmol), Fe₃O₄/SiO₂/PPA magnetic nanocatalyst (50 mg), solvent-free conditions, at 50 °C;

^bIsolated yield.

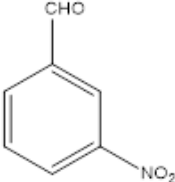
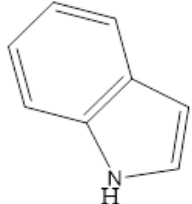
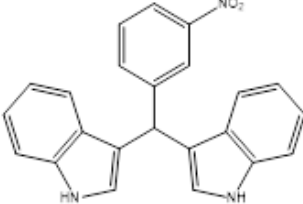
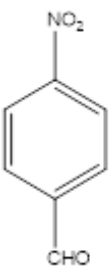
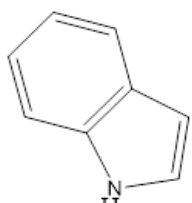
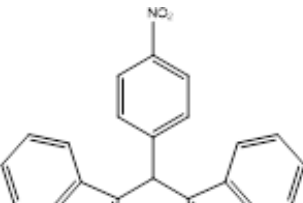
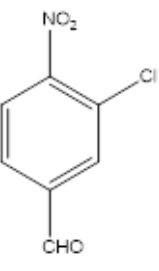
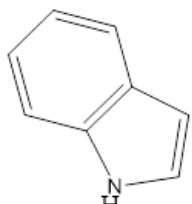
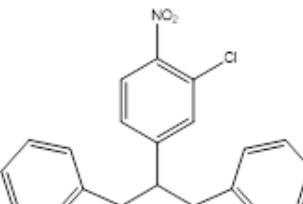
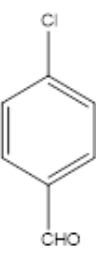
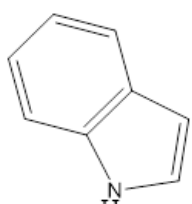
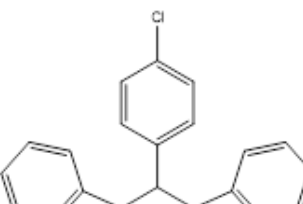
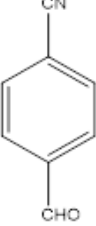
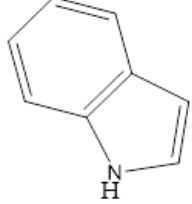
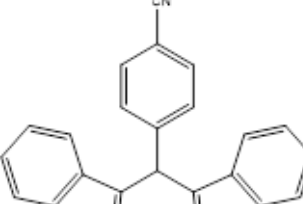
Continued of Table 5.

Entry	Aldehyde	2-Methylindol And Indol	Product	Time (min)	Yielda (%)
11				10	96
12				20	76
13				18	82
14				10	90
15				20	78

^aReaction conditions: aldehyde (1 mmol), indole or 2-methylindole (2 mmol), Fe₃O₄/SiO₂/PPA magnetic nanocatalyst (50 mg), solvent-free conditions, at 50 °C;

^bIsolated yield.

Continued of Table 5.

Entry	Aldehyde	2-Methylindol And Indol	Product	Time (min)	Yielda (%)
16				15	83
17				6	92
18				15	85
19				12	88
20				7	91

^aReaction conditions: aldehyde (1 mmol), indole or 2-methylindole (2 mmol), Fe₃O₄/SiO₂/PPA magnetic nanocatalyst (50 mg), solvent-free conditions, at 50 °C;

^bIsolated yield.

Continued of Table 5.

Entry	Aldehyde	2-Methylindol And Indol	Product	Time (min)	Yielda (%)
21				20	75
22				25	70
23				25	75
24				40	60
25				35	65

^aReaction conditions: aldehyde (1 mmol), indole or 2-methylindole (2 mmol), Fe₃O₄/SiO₂/PPA magnetic nanocatalyst (50 mg), solvent-free conditions, at 50 °C;

^bIsolated yield.

containing electron-withdrawing and electron-donating groups were efficiently condensed with indole derivatives. Also, it can be established that the presence of the electron-withdrawing groups (CN, NO₂) on the aromatic ring can increase the reaction rate and, as a result, the reaction times are decreased and the yields are increased whereas the electron-releasing group (OMe) possessed diverse effects. This indicates that the synthesis reaction of bis(indolyl)methanes are sensitive to the substituent groups on the aldehyde ring, with electron-withdrawing groups increasing the reaction rate and efficiency, and electron-donating groups decreasing these values.

3.2.3 Reaction mechanism

First, an acid catalyst Fe₃O₄/SiO₂/PPA, activates the carbonyl group in aldehyde derivative 1 and turns it into intermediate 4. This intermediate becomes intermediate 5 due to the increase of nucleophilicity of the first molecule of indole 2. In the following, intermediate 5 becomes intermediate 6 by tautomerization. By

dehydration of intermediate 6, azafulvenium salt 7 is formed. Then, intermediate 8 is formed by increasing the nucleophilicity of the second molecule of indole 1 to azafulvenium salt 7. At the end, the bis-indolylmethane product 3 is obtained by tautomerization of intermediate 8 (figure 10) [2].

3.2.4 Recyclability of the nanocatalyst

The magnetic nanocatalyst was recovered and reused multiple times in the model reaction to assess its recyclability. The recovery procedure involved separating the nanocatalyst using an external magnet after the reaction was completed, followed by washing the catalyst three times with ethanol before reuse in subsequent reactions. As illustrated in figure 11, the catalyst was successfully reused five times without a significant decline in catalytic activity.

Also, figure 12 presents the FT-IR spectra of recovered Fe₃O₄/SiO₂/PPA catalyst.

To emphasize the significance of the current study

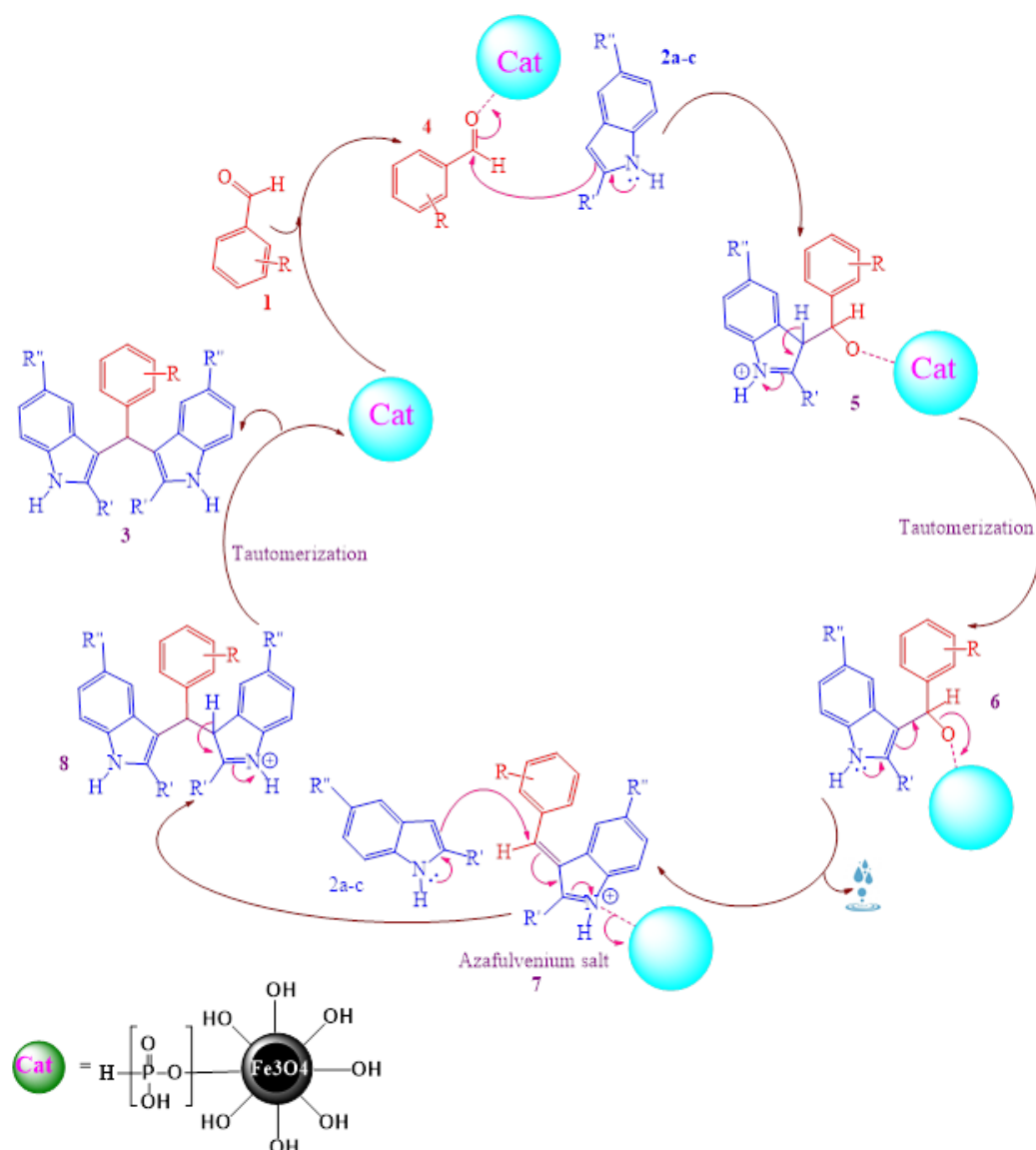


Figure 10. Proposed mechanism for the synthesis of bis(indolyl)methanes catalyzed by Fe₃O₄/SiO₂/PPA.

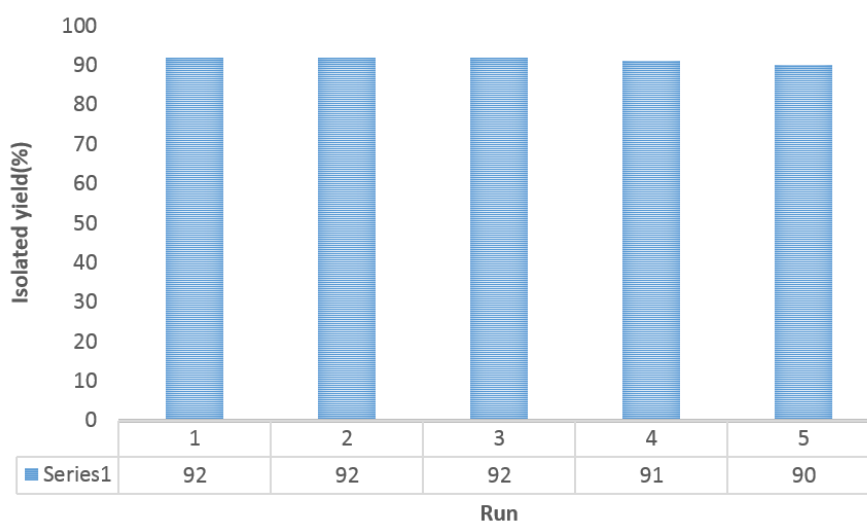


Figure 11. Recyclability of the nanocatalyst.

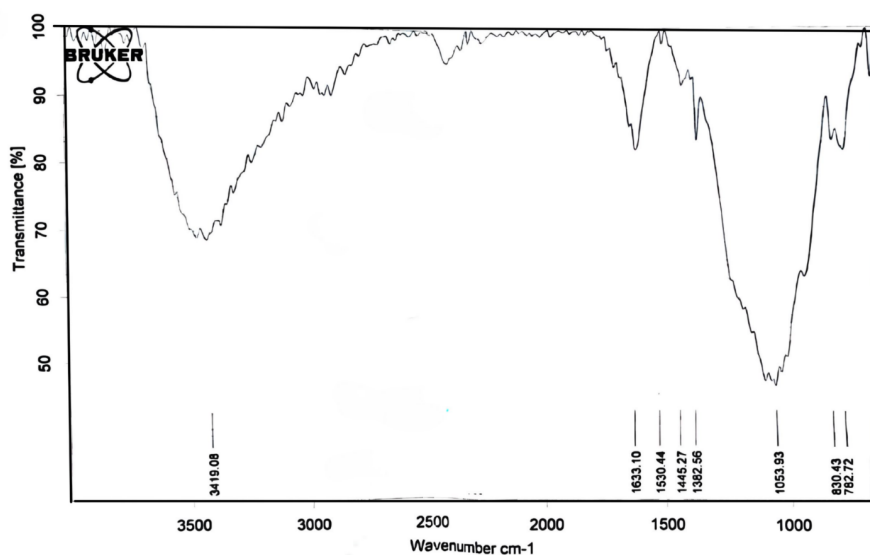


Figure 12. The FT-IR spectra of recovered $\text{Fe}_3\text{O}_4/\text{SiO}_2/\text{PPA}$ catalyst.

in comparison to previously reported findings, we have presented our results and reaction conditions for the synthesis of the target molecule (indole and benzaldehyde) alongside data from similar studies in Table 6. As

shown in this table, the $\text{Fe}_3\text{O}_4/\text{SiO}_2/\text{PPA}$ catalyst can be considered a suitable catalyst for both efficiency and reaction time.

Table 6. Comparison of this approach with further processes for the preparation of target molecule indole and benzaldehyde (Table 5, Entry 14)^a.

Entry	Reaction condition	Time (min)	Yield (%) ^b	Reported reference
1	$\text{Fe}_3\text{O}_4/\text{SiO}_2/\text{PPA}$ (50 Mg), Solvent free, 50 °C	10	90	This work
2	silica gel (50 mg), 100 °C	60	99	[59]
3	Sulfated zirconia (15 mol%), Solvent free, r.t.	360	36	[60]
4	PVPP-OTf (30 Mg), CH_3CN , r.t.	60	90	[61]
5	POCl_3 (1.1 mmol), DMF (4 mmol), 40 °C	300	55	[62]
6	MOF-891 (1 mol%), <i>m</i> -xylene, sonication	90	92	[63]
7	Chitosan supported ionic liquid (50 mol%), Ethanol, 50 °C	60	95	[64]

^abenzaldehyde (1.0 mmol), indole (2.0 mmol), and $\text{Fe}_3\text{O}_4/\text{SiO}_2/\text{PPA}$ magnetic nanocatalyst (50 mg), at 50 °C;

^bIsolated yield.

4. Conclusions

In summary, we report the synthesis of Fe₃O₄/SiO₂/PPA as a novel nanomagnetic solid acid catalyst, containing the PPA on the surface of Fe₃O₄/SiO₂ as the catalytic support. We prepared a green magnetic nanocatalyst. Using a simple methodology in this way, we first prepared nano-silica from the horsetail plant (*Equisetum arvense*), which is rich in silica. Then, we combined this compound with nano Fe₃O₄ to synthesize Fe₃O₄/SiO₂. Next, from the reaction of this compound with polyphosphoric acid (PPA), we synthesized Fe₃O₄/SiO₂/PPA magnetic nanocatalyst through a low-cost method. The structure of the synthetic catalyst was determined using various spectroscopic techniques. Then, bis(indolyl)methane products were synthesized from this catalyst during the reaction of indole or 2-methylindole with various aromatic and heteroaromatic aldehydes in solvent-free conditions and at a temperature of 50 °C. This method has many advantages such as using an efficient, cheap, environmentally friendly, magnetically recyclable nanocatalyst with straightforward isolation, no solvent use, short reaction time and high yields.

Acknowledgments

The authors are thankful to the Ayatollah Amoli Branch, Islamic Azad University, for the facilities provided to carry out research in chemistry research laboratory.

Supporting Information

The supporting data include products' spectral images of ¹H-NMR and ¹³C-NMR of products and TGA and BET analysis of the catalyst.

Funding

This work was supported by ongoing institutional funding. No additional grants to carry out or direct this particular research were obtained.

Authors contributions

All authors contributed equally to the conception, design, execution, and writing of this work. All authors read and approved the final manuscript.

Availability of data and materials

The authors declare that the data supporting the findings of this study are available within the paper.

Conflict of interests

The authors assert that they do not have any identifiable conflicting financial interests or personal relationships that might be perceived to influence the work presented in this paper.

References

- Osawa T and Namiki M. "Structure elucidation of streptindole a novel genotoxic metabolite isolated from intestinal bacteria." *Tetrahedron Lett.* 1983; 24:4719–22. DOI: [10.1016/S0040-4039\(00\)86237-1](https://doi.org/10.1016/S0040-4039(00)86237-1)
- Bavafa M, Vahdat SM, and Khaksar S. "Nano γ -Al₂O₃: Enhancement of catalytic performance in the synthesis of Bis (Indolyl) Methanes." *Int. J. Nano Dimens.* 2022; 13:227–34. DOI: [10.22034/ijnd.2022.687824](https://doi.org/10.22034/ijnd.2022.687824)
- Garbe TR, Kobayashi M, Shimizu N, Takesue N, Ozawa M, and Yukawa H. "Indolyl Carboxylic Acids by Condensation of Indoles with α -Keto Acids." *J. Nat. Prod.* 2000; 63:596–598. DOI: [10.1021/np990517s](https://doi.org/10.1021/np990517s)
- Shiri M, Zolfigol MA, Kruger HG, and Tanbakouchian Z. "Bis- and Trisindolylmethanes (BIMs and TIMs)." *Chem Rev.* 2010; 110:2250–93. DOI: [10.1021/cr900195a](https://doi.org/10.1021/cr900195a)
- Kamal A, Naseer M, Khan A, Reddy KS, Srikanth Y, Ahmed SK, Kumar KP, and Murthy U. "An efficient synthesis of bis(indolyl)methanes and evaluation of their antimicrobial activities." *J. Enzyme Inhib. Med. Chem.* 2009; 24:559–565. DOI: [10.1080/14756360802292974](https://doi.org/10.1080/14756360802292974)
- Bharate SB, Bharate JB, Khan S, Tekwani B, Jacob MR, Mudududdla R, Yadav R, Singh B, Sharma P, Maiy S, Singh B, Khan I, and Vishwakarma R. "Discovery of 3,3'-diindolylmethanes as potent antileishmanial agents." *Eur. J. Med. Chem.* 2013; 63:435–43. DOI: [10.1016/j.ejmech.2013.02.024](https://doi.org/10.1016/j.ejmech.2013.02.024)
- Saleh E, Firoz K, Uthirapathy S, Asiri M, Kundlas RMMM, Kumar V, Ray S, Yousif ZS, and Salman HR. "Recent advances in catalytic approaches for the synthesis of 3-substituted indoles: Mechanisms and strategies." *ACS Omega.* 2025; 16:12255–90. DOI: [10.1039/D5RA00871A](https://doi.org/10.1039/D5RA00871A)
- Ziarani GM, Moradi R, Ahmadi T, and Lashgari N. "Recent advances in the application of indoles in multicomponent reactions." *RSC Advances.* 2018; 22:12069–103. DOI: [10.1039/C7RA13321A](https://doi.org/10.1039/C7RA13321A)
- Ahmad T, Khan S, and Ullah N. "Recent Advances in the Catalytic Asymmetric Friedel-Crafts Reactions of Indoles." *ACS Omega.* 2022; 7:3544635485. DOI: [10.1021/acsomega.2c05022](https://doi.org/10.1021/acsomega.2c05022)
- Teli P, Soni S, and Teli S. "Unlocking Diversity: From Simple to Cutting-Edge Synthetic Methodologies of Bis(indolyl)methanes." *Top Curr Chem.* 2024; 382:619–29. DOI: [10.1007/s41061-024-00454-z](https://doi.org/10.1007/s41061-024-00454-z)
- Khanna L, Mansi, Yadav S, Misra N, and Khanna P. "In water" synthesis of bis(indolyl)methanes: a review. *Synthetic Communications* 2021; 51:2892–2923. DOI: [10.1080/00397911.2021.1957113](https://doi.org/10.1080/00397911.2021.1957113)
- Kamboj P and Tyagi V. "A recent update on the environment friendly methodologies to synthesize bis(indolyl)methane and 3,3-di(3-indolyl)-2-indolone derivatives." *Tetrahedron* 2023; 148:133679. DOI: [10.1016/j.tet.2023.133679](https://doi.org/10.1016/j.tet.2023.133679)

13. Kundu A and Mukhopadhyay C. "Synthetic Strategies of Highly Bioactive Scaffold Bis(indolyl)methane Under Greener Condition-A Comprehensive Review." *Medicinal Chemistry* 2024; 25:779–812. DOI: [10.2174/0115680266319238240821080203](https://doi.org/10.2174/0115680266319238240821080203)
14. Bedi P, Kaur R, Bose R, Pakhira B, Roy M, and Pramanik T. "Recent Advancement in the Green Synthesis of Bis(indolyl) Methane via One-pot Multicomponent Condensation Strategy-A Mini Review." *Oriental Journal of Chemistry* 2024; 40:2231–5039. DOI: [10.13005/ojc/400502](https://doi.org/10.13005/ojc/400502)
15. Arjun-Chavan K, Chavan P, Kumar A, and Erande R. "Cascade approach to synthesize BIMs and analogues in different nucleophilic conditions." *Tetrahedron Lett.* 2024; 148:155248. DOI: [10.1016/j.tetlet.2024.155248](https://doi.org/10.1016/j.tetlet.2024.155248)
16. Chavan K, Shukla M, Nath-Singh-Chauhan A, Maji S, Mali G, Bhattacharyya S, and Erande R. "Effective Synthesis and Biological Evaluation of Natural and Designed Bis(indolyl)methanes via Taurine-Catalyzed Green Approach." *ACS Omega.* 2022; 7:10438–46. DOI: [10.1021/acsomega.1c07258](https://doi.org/10.1021/acsomega.1c07258)
17. Srivastava A, Agarwal A, Gupta S, and Jain N. "Graphene oxide decorated with Cu(i)Br nanoparticles: a reusable catalyst for the synthesis of potent bis(indolyl)methane based anti HIV drugs." 2016; *RSC Adv.*:23008–11. DOI: [10.1039/C6RA02458K](https://doi.org/10.1039/C6RA02458K)
18. Ge X, Yannai S, Rennert G, Gruener N, and Fares F. "3,3'-Diindolylmethane Induces Apoptosis in Human Cancer Cells." *BBRC* 1996; 228:153–8. DOI: [10.1006/bbrc.1996.1631](https://doi.org/10.1006/bbrc.1996.1631)
19. Contractor R, Samudio I, Estrov Z, Harris D, McCubrey J, Safe S, Andreeff M, and Konopleva M. "A Novel Ring-Substituted Diindolylmethane, 1,1-Bis[3'-(5-Methoxyindolyl)]-1-(p-t-Butylphenyl) Methane, Inhibits Extracellular Signal-Regulated Kinase Activation and Induces Apoptosis in Acute Myelogenous Leukemia." *Cancer Res.* 2005; 65:2890–2898. DOI: [10.1158/0008-5472.CAN-04-3781](https://doi.org/10.1158/0008-5472.CAN-04-3781)
20. Lee J. "3,3'-Diindolylmethane Inhibits TNF- α -and TGF- β -Induced Epithelial–Mesenchymal Transition in Breast Cancer Cells." *Nutr Cancer.* 2019; 71:992–1006. DOI: [10.1080/01635581.2019.1577979](https://doi.org/10.1080/01635581.2019.1577979)
21. Jamsheena V, Shilpa G, Saranya J, Harry NA, Lankalapalli RS, and Priya S. "Anticancer activity of synthetic bis(indolyl)methane-ortho-biaryls against human cervical cancer (HeLa) cells." *Chem Biol Interact.* 2016; 247:11–21. DOI: [10.1016/j.cbi.2016.01.017](https://doi.org/10.1016/j.cbi.2016.01.017)
22. Pramanik A and Bharb S. "Silica-sulfuric acid and alumina-sulfuric acid: Versatile supported Brønsted acid catalysts." *New Journal of Chemistry* 2021; 45:16355–88. DOI: [10.1039/D1NJ02887A](https://doi.org/10.1039/D1NJ02887A)
23. Baghernejad B. "Silica Sulfuric Acid (SSA): An Efficient and Heterogeneous Catalyst for Organic Transformations." *Mini-Reviews in Organic Chemistry* 2011; 8:91–102. DOI: [10.2174/157019311793979963](https://doi.org/10.2174/157019311793979963)
24. Mohammadi M, Khodamorady M, Tahmasbi B, Bahrami K, and A.Ghorbani-Choghamarani. "Boehmite nanoparticles as versatile support for organic–inorganic hybrid materials: Synthesis, functionalization, and applications in eco-friendly catalysis." *Journal of Industrial and Engineering Chemistry* 2021; 97:1–78. DOI: [10.1016/j.jiec.2021.02.001](https://doi.org/10.1016/j.jiec.2021.02.001)
25. Nikseresht A, Karami M, and Mohammadi M. "Phosphotungstic Acid-Supported Hercynite: A Magnetic Nanocomposite Catalyst for the Selective Esterification of Chloroacetic Acid." *Langmuir.* 2024; 40:18512–24. DOI: [10.1021/acs.langmuir.4c01763](https://doi.org/10.1021/acs.langmuir.4c01763)
26. Esmaili S, Khazaei A, Ghorbani-Choghamarani A, and Mohammadi M. "Silica sulfuric acid coated on SnFe₂O₄ MNPs: Synthesis, characterization and catalytic applications in the synthesis of polyhydroquinolines." *RSC Advances* 2022; 23:14397–410. DOI: [10.1039/D2RA01202B](https://doi.org/10.1039/D2RA01202B)
27. Mohammadi M and Ghorbani-Choghamarani A. "Hercynite silica sulfuric acid: A novel inorganic sulfurous solid acid catalyst for one-pot cascade organic transformations." *RSC Advances* 2022; 40:26023–41. DOI: [10.1039/D2RA03481F](https://doi.org/10.1039/D2RA03481F)
28. Mohammadi M and Ghorbani-Choghamarani A. "Synthesis and characterization of novel hercynite@sulfuric acid and its catalytic applications in the synthesis of polyhydroquinolines and 2,3-dihydroquinazolin-4(1H)-ones." *RSC Advances* 2022; 5:2770–87. DOI: [10.1039/D1RA07381H](https://doi.org/10.1039/D1RA07381H)
29. Kazemi M and Mohammadi M. Magnetically Recoverable Catalysts: Catalysis in Synthesis of Polyhydroquinolines.
30. Vahdat S, Khaksar S, and Bagheri S. "An efficient one-pot synthesis of bis(indolyl)methanes catalyzed by ionic liquid with multi-SO₃H groups under ambient temperature in water." *World Appl. Sci. J.* 2011; 15:877–884
31. Firouzabadi H, Iranpoor N, and Jafari A. "Aluminumdodecatungstophosphate (AIPW₁₂O₄₀), a versatile and a highly water tolerant green Lewis acid catalyzes efficient preparation of indole derivatives." *J. Mol. Catal. A Chem.* 2006; 244:168–72. DOI: [10.1016/j.molcata.2005.09.005](https://doi.org/10.1016/j.molcata.2005.09.005)

32. Ghorbani-Vaghei R and Veisi H. "Poly(N,N'-dichloro-N-ethyl-benzene-1, 3-disulfonamide) and N,N,N',N'-tetrachlorobenzene-1,3-disulfonamide as novel catalytic reagents for synthesis of bis-indolyl, tris-indolyl, di(bis-indolyl), tri(bis-indolyl) and tetra(bis-indolyl)methanes under solid-state, solvent and water conditions." *J. Braz. Chem. Soc.* 2010; 21:193–201. DOI: [10.1590/S0103-50532010000200002](https://doi.org/10.1590/S0103-50532010000200002)
33. Seyedi N, Khabazzadeh H, and Saidi K. "Cu_{1.5}PMo₁₂O₄₀ as an efficient, mild and heterogeneous catalyst for the condensation of indole with carbonyl compounds." *Mol. Divers.* 2009; 13:337–342. DOI: [10.1007/s11030-009-9120-5](https://doi.org/10.1007/s11030-009-9120-5)
34. Sheikhshoae I, Khabazzadeh H, and Saeid-Nia S. "Iron(III)(salen)Cl as an efficient catalyst for synthesis of bis(indolyl)methanes." *Transition Met Chem.* 2009; 34:463–466. DOI: [10.1007/s11243-009-9217-9](https://doi.org/10.1007/s11243-009-9217-9)
35. Sheng SR, Wang Q, Ding Y, Liu X, and Cai M. "Synthesis of Bis(indolyl)methanes Using Recyclable PEG-Supported Sulfonic Acid as Catalyst." *Catal Lett.* 2009; 128:418–22. DOI: [10.1007/s10562-008-9767-z](https://doi.org/10.1007/s10562-008-9767-z)
36. Rahimizadeh M, Bakhtiarpoor Z, Eshghi H, Pordel M, and Rajabzadeh G. "TiO₂ nanoparticles: An efficient heterogeneous catalyst for synthesis of bis(indolyl)methanes under solvent-free conditions." *Computational and Theoretical Chemistry* 2009; *Monatsh Chem.*:1465–1469. DOI: [10.1007/s00706-009-0205-8](https://doi.org/10.1007/s00706-009-0205-8)
37. Ma Z, Han H, Zhou Z, and Nie J. "SBA-15-supported poly(4-styrenesulfonyl(perfluorobutylsulfonyl)imide) as heterogeneous Brønsted acid catalyst for synthesis of diindolylmethane derivatives." *J. Mol. Catal. A: Chem.* 2009; 21:46–53. DOI: [10.1016/j.molcata.2009.06.021](https://doi.org/10.1016/j.molcata.2009.06.021)
38. Vahdat S, Khaksar S, and Bagheri S. "Sulfonated Organic Heteropolyacid Salts: Recyclable Green Solid Catalysts for the Highly Efficient and Green Synthesis of Bis(indolyl)methanes in Water." *Lett. Org. Chem.* 2012; 9:138–44. DOI: [10.2174/157017812800221690](https://doi.org/10.2174/157017812800221690)
39. Patil V, Dere G, Rege P, and Patil J. "Synthesis of Bis(indolyl) Methanes in Catalyst- and Solvent-Free Reaction." *Synth. Commun.* 2012; 41:736–47. DOI: [10.1080/00397911003642690](https://doi.org/10.1080/00397911003642690)
40. Greger M and Landberg T. "Equisetum arvense as a silica fertilizer." *PPB* 2024; 210:108606. DOI: [10.1016/j.plaphy.2024.108606](https://doi.org/10.1016/j.plaphy.2024.108606)
41. Mohtasham NH and Gholizadeh M. "Nano silica extracted from horsetail plant as a natural silica support for the synthesis of H₃PW₁₂O₄₀ immobilized on aminated magnetic nanoparticles (Fe₃O₄@SiO₂-EP-NH-HPA): A novel and efficient heterogeneous nanocatalyst for the green one-pot synthesis of pyrano[2,3-c]pyrazole derivatives." *Chem. Intermed.* 2020; 46:3037–66. DOI: [10.1007/s11164-020-04133-8](https://doi.org/10.1007/s11164-020-04133-8)
42. Ahmadi E, Khazaei A, and Akbarpour T. "[Fe₃O₄@CQD@Si(OEt)(CH₂)₃NH@CC@Ad@SO₃H]⁺Cl⁻: As a new, efficient, magnetically separable and reusable heterogeneous solid acid catalyst for the synthesis of 5-amino-1,3-diphenyl-1H-pyrazole 4-carbonitril and pyrano[2,3-c] pyrazole derivatives." *Chem. Intermed.* 2023; 49:2099–122. DOI: [10.1007/s11164-022-04919-y](https://doi.org/10.1007/s11164-022-04919-y)
43. Carneiro DM, Jardim TV, Araújo YL, Arantes AC, Sousa AC de, Barroso WKS, and Lima AL. "Equisetum arvense: New Evidences Supports Medical use in Daily Clinic." *Pharmacogn Rev.* 2019; 13:50–8. DOI: [10.5530/phrev.2019.2.4](https://doi.org/10.5530/phrev.2019.2.4)
44. Silva RMF da Costa e, Diniz IMA, and Fonte Ferreira JM da. "Extracts and Composites of Equisetum for Bone Regeneration Living reference work entry." 2022; Springer. *Cham.*:1–27. DOI: [10.1007/978-3-030-97415-2_31-1](https://doi.org/10.1007/978-3-030-97415-2_31-1)
45. Karami N, Mohammadpour A, Samaei M, Amani A, Dehghani M, S. Varma R er, and Sahu JN. "Green synthesis of sustainable magnetic nanoparticles Fe₃O₄ and Fe₃O₄-chitosan derived from Prosopis farcta biomass extract and their performance in the sorption of lead(II)." *Int. J. Biol. Macromol.* 2024; 254:127663. DOI: [10.1016/j.ijbiomac.2023.127663](https://doi.org/10.1016/j.ijbiomac.2023.127663)
46. Chen L, Gao T, Wu X, He M, Wang X, Teng F, and Li Y. "Polycarboxylate functionalized magnetic nanoparticles Fe₃O₄@SiO₂@CS-COOH: Preparation, characterization, and immobilization of bovine serum albumin." *Int. J. Biol. Macromol.* 2024; 260:129617. DOI: [10.1016/j.ijbiomac.2024.129617](https://doi.org/10.1016/j.ijbiomac.2024.129617)
47. Elshimy A, Mobarak M, Ajarem J, Maooda S, Bonilla-Petriciolet A, Li Z, Korany M, Ammar D, Awad D, Elberbash S, and Seliem M. "Sodium alginate-modified alkali-activated eggshell/Fe₃O₄ nanoparticles: A magnetic bio-based spherical adsorbent for cationic dyes adsorption." *Int. J. Biol. Macromol.* 2024; 256:128528. DOI: [10.1016/j.ijbiomac.2023.128528](https://doi.org/10.1016/j.ijbiomac.2023.128528)
48. Mathew A, Jayaprakash A, Ratnamma AM, Veetil SP, Hamza ZP, Sivarajan A, Kochappan RP, Thathuveetil RK, Jose J, Jacob K, and Saidu FK. "Evaluation of the catalytic and in-vitro anticancer potential of Gold nanoparticles synthesized using clammy cherry (Cordia Obliqua Willd)." *Int. J. Nano Dimens.* Accepted Manuscript. 2025. DOI: [10.57647/j.ijnd.2025.1604.30](https://doi.org/10.57647/j.ijnd.2025.1604.30)

49. Acharya S, Behera A, A. CS SV, and Thiya-garajan R. "Thirunavukkarasu Chinnasamy Green-synthesized Titanium Dioxide nanoparticles with Pyrogallol functionalization: A novel approach using cow dung extract for anticancer applications." *Int. J. Nano Dimens* 2025. doi: [10.57647/j.ijnd.2025.1603.17](https://doi.org/10.57647/j.ijnd.2025.1603.17).
50. Shaik R, Buggana A, Thalari V, Rani S, Bandari EK, and Golla N. "Green synthesis, characterization, and biological activities of copper nanoparticles using *Clitoria ternatea* leaf extract." *Int. J. Nano Dimens.* 2025; 16:162505. doi: [10.57647/j.ijnd.2025.1601.05](https://doi.org/10.57647/j.ijnd.2025.1601.05)
51. Yazdani S, Hatami M, and Vahdat S. "The chemistry concerned with the sonochemical-assisted synthesis of CeO₂/poly(amic acid) nanocomposites." *Turk. J. Chem.* 2014; 38:388–401. doi: [10.3906/kim-1306-33](https://doi.org/10.3906/kim-1306-33)
52. Hosseini-Mohtasham N and Gholizadeh M. "Horsetail plant (*Equisetum arvense*) and horsetail plant ash: application and comparison of their catalytic activities as novel and natural porous lewis acid catalysts for the one pot green synthesis of 2-amino-4H-chromene derivatives under solvent free conditions." *JICS* 2020; 17:397–409. doi: [10.1007/s13738-019-01777-1](https://doi.org/10.1007/s13738-019-01777-1)
53. Hassankhani A, Sadeghzadeh S, and Zhiani R. "C-C and C-H coupling reactions by Fe₃O₄/KCC-1/APTPOSS supported palladium-salen-bridged ionic networks as a reusable catalyst." *RSC Adv* 2018; 8:8761–9. doi: [10.1039/C8RA00485D](https://doi.org/10.1039/C8RA00485D)
54. An D, Guo Y, Zhu Y, and Wang Z. "A Green Route to Preparation of Silica Powders with Rice Husk Ash and Waste Gas." *J. Chem. Eng.* 2010; 162:509–14. doi: [10.1016/j.cej.2010.05.052](https://doi.org/10.1016/j.cej.2010.05.052)
55. Adam F, Kandasamy K, and Balakrishnan S. "Iron incorporated heterogeneous catalyst from rice husk ash." *Journal of Colloid and Interface Science* 2006; 304:137–43. doi: [10.1016/j.jcis.2006.08.051](https://doi.org/10.1016/j.jcis.2006.08.051)
56. Amarloo F, Zhiani R, and Mehrzad J. "Novel Fe₃O₄/SiO₂/PPA Magnetic Nanoparticles: Preparation, Characterization, and First Catalytic Application to the Solvent-Free Synthesis of Tetrahydrobenzo[a]xanthene-11-ones." *Russ. J. Org. Chem.* 2019; 55:1584–1590. doi: [10.1134/S1070428019100191](https://doi.org/10.1134/S1070428019100191)
57. Tayebee R, Pejhan A, Ramshini H, Maleki B, Erfaninia N, Tabatabaie Z, and Esmaeili E. "Equisetum arvense as an abundant source of silica nanoparticles. SiO₂/H₃PW₁₂O₄₀ nanohybrid material as an efficient and environmental benign catalyst in the synthesis of 2-amino-4Hchromenes under solvent-free conditions." *Appl Organometal Chem.* 2017 :e3924. doi: [10.1002/aoc.3924](https://doi.org/10.1002/aoc.3924)
58. Habibi D, Kaamyabi S, and Hazarkhani H. "Fe₃O₄ nanoparticles as an efficient and reusable catalyst for the solvent-free synthesis of 9,9-dimethyl-9,10-dihydro-8H-benzo[a]xanthene-11(12H)-ones." *Chinese Journal of Catalysis* 2015; 36:362–6. doi: [10.1016/S1872-2067\(14\)60238-2](https://doi.org/10.1016/S1872-2067(14)60238-2)
59. Mendes S, Thurow S, Fortes M, Pentead F, Lenardao E, Alves D, Perin G, and Jacob R. "Synthesis of bis(indolyl)methanes using silica gel as an efficient and recyclable surface." *Tetrahedron Lett.* 2012; 53:5402–6. doi: [10.1016/j.tetlet.2012.07.118](https://doi.org/10.1016/j.tetlet.2012.07.118)
60. Chen G, Guo C, Qiao H, Ye M, Qiu X, and Yue C. "Well-dispersed sulfated zirconia nanoparticles as high-efficiency catalysts for the synthesis of bis(indolyl)methanes and biodiesel." *Catal. Commun.* 2013; 41:70–4. doi: [10.1016/j.catcom.2013.07.006](https://doi.org/10.1016/j.catcom.2013.07.006)
61. Khaksar S, Tajbakhsh M, and Gholami M. "Polyvinylpyrrolidone-supported triflic acid (PVPP-OTf) as a new, efficient, and recyclable heterogeneous catalyst for the synthesis of bis-indolyl methane derivatives." *C. R. Chim.* 2014; 17:30–4. doi: [10.1016/j.crci.2013.07.014](https://doi.org/10.1016/j.crci.2013.07.014)
62. Veisi H, Ataee M, Darabi-Tabar P, Amiri E, and Faraji A. "One-pot conversion of aromatic compounds to the corresponding bis(indolyl)methanes by the Vilsmeier-Haack reaction." *C. R. Chim.* 2014; 17:305–9. doi: [10.1016/j.crci.2013.09.011](https://doi.org/10.1016/j.crci.2013.09.011)
63. Nguyen H, Nguyen T, Nguyen P, and Tran P. "A highly active copper-based metal-organic framework catalyst for a friedel-crafts alkylation in the synthesis of bis(indolyl)methanes under ultrasound irradiation." *Arab. J. Chem.* 2020; 13:1377–85. Available from: <http://creativecommons.org/licenses/by-nc-nd/4.0/>
64. Patel G, Kure A, Mandawad G, Hote B, and Konda S. "Chitosan supported ionic liquid (CSIL): An excellent catalyst for one-pot synthesis of bis(indolyl)methanes." *Result Chem.* 2022; 4:100436. doi: [10.1016/j.rechem.2022.100436](https://doi.org/10.1016/j.rechem.2022.100436)